Edge-Coupling of O-Band InP Etched-Facet Lasers to Polymer Waveguides on SOI by Micro-Transfer-Printing

Ruggero Loi, Simone Iadanza, Brendan Roycroft, James O'Callaghan, Lei Liu, Kevin Thomas, Agnieszka Gocalinska, Emanuele Pelucchi, Alexander Farrell, Steven Kelleher, Raja Fazan Gul, António José Trindade, David Gomez, Liam O'Faolain, and Brian Corbett

***Abstract*— O-band InP etched facets lasers were heterogeneously integrated by micro-transfer-printing into a 1.54 μm deep recess created in the 3 μm thick oxide layer of a 220 nm SOI wafer. A 7 x 1.5 μm^2 cross-section, 2 mm long multimode polymer waveguide was aligned to the ridge post-integration by e-beam lithography with <0.7 μm lateral misalignment and incorporated a tapered silicon waveguide. A 170 nm thick metal layer positioned at the bottom of the recess adjusts the vertical alignment of the laser and serves as a thermal via to sink the heat to the Si substrate. This strategy shows a roadmap for active polymer waveguide-based photonic integrated circuits.**

***Index Terms*— Heterogeneous integration, III-V semiconductors laser, silicon photonics, polymer waveguides.**

I. Introduction

SILICON photonics exploits the high-volume manufacturing capability of the CMOS microelectronics industry [1], [2] offering low-cost photonic circuits. The Silicon-on Insulator (SOI) platform of 220 nm of Si on 2 μm of SiO_2 on a silicon substrate provides compact waveguides due to the high refractive index contrast between the Si waveguide core and the SiO_2 cladding. Alternatively, a thicker buried oxide (BOX) can be used for waveguides with lower refractive index such as those based on polymers. Silicon photonic integrated circuits for application in the telecommunication wavelength domain of 1300–1600 nm benefit from the use of InP-based materials as these provide the most mature direct band-gap structures for light amplification, modulation and detection [3]. The light-coupling between the InP component and the SOI waveguide can be achieved by edge-coupling which offers broad band, polarization-agnostic low coupling losses of less than 1 dB [4]. The approach does not require the definition of tapers on the InP reducing its footprint and in turn the use of expensive material. Mode mismatch is the major source of the insertion losses in edge-coupling, which is overcome by the use of mode size converters (MSC) and tight alignment tolerances. Reflective semiconductor optical amplifier (RSOA) chips have been edge-coupled to silicon photonics in external cavity laser configuration, with no need of MSC nor wafer bonding but still needing precise alignment [5], [6]. The edge coupling of fully packaged lasers on chip has been reported [7]–[10]. The integration of active photonic devices on SOI has been successfully accomplished by die/wafer bonding [11]–[16] and more recently by micro-transfer-printing (μTP) [17]–[19]. In particular, InP-based Fabry-Perot and DFB lasers, LEDs, and photodiodes have been heterogeneously integrated with silicon photonics by using μTP [20]–[23]. Heterogeneous integration by μTP offers high-throughput, parallel and scalable transfer of devices or dies of material in the desired locations on the integration platform. The technique offers planar placement accuracy of less than 1.5 μm (over 3σ) for arrays of dies or devices and less than 1 μm tolerant alignments for single posts [24]–[26] by utilizing pattern recognition. Highly dense arrays of transfer-printable coupons can be accommodated on the source wafer. μTP permits the heterogenous integration of fully pre-fabricated or partially processed devices, enabling a known-good die micro assembly approach with different elements that can be integrated to a common platform. The only requirement for the bonding surfaces is that they are locally flat and co-planar. μTP allows integration onto both rigid and flexible substrates, inside recesses, with and without adhesive layers [27], [28].

The edge-coupling of InP-based etched-facet lasers to silicon photonics waveguides by heterogeneous integration into recesses defined on the SOI has been recently demonstrated through μTP [29]–[31]. In this case the devices are printed directly on the Si substrate and use an n-InP cladding layer of

Manuscript received June 27, 2019; revised November 8, 2019; accepted December 2, 2019. Date of publication December 9, 2019; date of current version December 26, 2019. This work was supported in part by the Science Foundation Ireland under Grant 12/RC/2276 (IPIC), 15/IA/2864, in part by the European Union's Horizon 2020 Research and Innovation Programme under Grant 645314 (TOP-HIT), and in part by the European Research Council Starting Grant 337508 (DANCER) under Grant 780240 (REDFINCH). *(Corresponding author: Ruggero Loi.)*

R. Loi and L. Liu were with the Tyndall National Institute, University College Cork, Cork, T12 R5CP Ireland; They are now with X-Celeprint Limited, Cork, T12 R5CP Ireland (e-mail: rloi@x-celeprint.com).

S. Iadanza and L. O'Faolain are with the Cork Institute of Technology, Cork, T12 P928 Ireland.

B. Roycroft, J. O'Callaghan, K. Thomas, A. Gocalinska, E. Pelucchi, and B. Corbett are with the Tyndall National Institute, University College Cork, Cork, T12 R5CP Ireland.

A. Farrell, S. Kelleher, R. F. Gul, A. J. Trindade, and D. Gomez are with X-Celeprint Limited, Cork, T12 R5CP Ireland.

Color versions of one or more of the figures in this article are available online at http://ieeexplore.ieee.org.

Digital Object Identifier 10.1109/JQE.2019.2958365

tailored thickness for the alignment of the emitting waveguide to a trident MSC defined on the SOI. Mode size conversion is required as the mode size in the laser waveguide is mismatched to that of the SOI waveguide. Recesses are etched at the ends of the SOI waveguide for reduced longitudinal misalignment. Printing in contact to the Si substrate provides reduced thermal impedance to the laser [32]. A similar approach can be applied for edge-coupling an InP laser to a polymer waveguide defined on the oxide layer of an SOI [33]. The light injected into the polymer waveguide can be used to power polymer-based photonic circuits [34], [35] or it can be next evanescently coupled to the SOI to create hybrid polymer-SOI photonics [36], [37].

This work reports the first O-band Fabry-Perot InP laser heterogeneously integrated into a recess on the SOI by μTP and edge-coupled to an SU8 polymer waveguide. The process allows accurate engineering for the waveguide alignments where an intermediate metal layer deposited at the bottom of the recess calibrates the alignment along the vertical axis with sub-micron precision and sinks the heat produced by the device to the Si substrate. The configuration provides reduced thermal impedance compared to devices integrated on the SOI layer [32], a different geometry of the thermal via is simulated here and shows how the thermal sink could be further improved.

II. Integration Strategy

An edge-coupled laser is to be integrated inside a recess etched into the SOI in order to achieve vertical alignment of the waveguides. The recess requires vertical sidewalls with mirror quality defined at the end of the SOI for maximum coupling efficiency which must not damage the delicate tip of any tapers defined on the SOI for mode size conversion [29, 30]. Careful choice of alignment marks is required for accurate positioning.

A. Layout

As the position of the InP die along the vertical axis inside the recess has to be tailored, different configurations have been studied [Fig. 1]. The first layout is with the recess etched to the Si substrate of the SOI wafer and the laser printed directly on the substrate, the arrangement offers the best thermal sink as the bottom of the device is in direct contact to the substrate [32]. In this case a >2 μm thick n-InP layer of calibrated thickness is required to achieve vertical alignment of the laser waveguide to the SOI waveguide [Fig. 1(a)]. A tailored and thick n-InP layer increases the epitaxial growth costs and makes the fabrication of the devices more challenging due to the increased thickness of the coupons. Alternatively, for a general n-InP layer thickness, a metal layer of calibrated thickness can be evaporated at the bottom of the recess on the Si substrate with $\sim$10 nm tolerance [Fig. 1(b)]. The strategy would increase the thermal sink as the gold has higher thermal conductivity than InP [32], but evaporation of thick metal layers can be expensive and require extra care in the preparation of the Si surface and in the metal deposition parameters for achieving flat and smooth surfaces that are essential for achieving adhesive-less printing or bonding with thin ($<$ 50 nm) adhesive layers. Imperfections or residual materials present on the starting surfaces or high rate metal evaporations can lead to metal seeding effects which create protrusions up to hundreds of nm in diameter on the final surface. These defects require the coupons to be printed with a thick adhesive layer which affects the vertical alignment of the coupon and the thermal impedance [32].

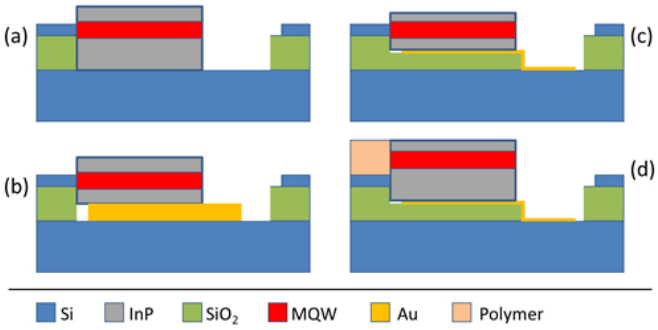

Fig. 1. Possible configurations for edge-coupling of a laser printed in a recess. (a) A laser die with an n-InP layer of calibrated thickness aligned to the SOI and in direct contact to the Si substrate. (b) A laser aligned to the SOI with an intermediate metal layer of calibrated thickness. (c) A laser printed in a recess of calibrated depth where a thin intermediate metal layer provides fine vertical alignment to the SOI and heat sink to the Si substrate. (d) Same layout as (c) for light coupling to a polymer waveguide.

Another option is to calibrate the recess depth into the buried oxide layer of the SOI and then adjust the vertical alignment of the coupon by evaporating an appropriate thin ($<$200 nm) metal layer at the bottom of the recess [Fig. 1(c)]. The metal layer works as an electrical contact and it can be connected to the Si substrate to act as a thermal via for enhanced heat dissipation. The laser integrated in the recess has the bottom closer to the Si substrate and then reduced thermal impedance compared to a laser printed on the SOI [32]. This strategy does not require either a n-InP layer of fixed thickness nor the evaporation of a thick metal layer.

The same strategies can be applied to edge-couple the laser to a polymer waveguide sitting on a cladding layer [Fig. 1(d)]. The layout reported in Fig 1(d) was designed for edge-coupling O-band InP lasers to a mode matched single mode polymer waveguide. One of the main advantages of the layout is the full butt coupling of the polymer waveguide to the facet which removes any air spacing and undesired Fabry-Perot resonances and the requirement to apply refractive-index-matched in-fillers, usually difficult to process. Full butt-coupling and accurate vertical alignment makes mode matching between the laser and the polymer waveguide easier compared to printing the laser at the top of the SOI and adjust the thickness of the polymer to align the waveguides. The polymer waveguide can act as an optical link to other optical functions of a photonic circuit or it can be used to evanescently couple the light to a tapered SOI waveguide for hybrid polymer-SOI photonics [35] or to realize advanced lasers [6]. The configuration allows the recess facet to be positioned far from the tip of the SOI taper, preventing damaging the taper during the etch process. The etched facets lasers do not require fabrication of tapers on the III-V reducing complexity of fabrication.

TABLE I

WAIST SIZE OF THE LASER TM MODE ALONG THE HORIZONTAL AND VERTICAL AXIS, FOR THE 2 μm WIDE RIDGE LASERS FABRICATED

Mode-size	Horizontal (μm)	Vertical (μm)
$w_0(1/e^2)$	1.625	0.578

B. Light Edge-Coupling Model

The edge-coupling strategy was chosen to couple the light emitted by the laser waveguide to a polymer waveguide. The highest potential coupling efficiency with this configuration is achieved when the laser mode field is matched to that of the waveguide in size and in phase. Accurate (<1 μm) positional alignment must be usually achieved in order to obtain <1 dB injection loss when coupling the light from the device to the waveguide.

The fundamental mode of the lasers fabricated as 2 μm wide ridge waveguides on an epitaxial structure emitting at 1340 nm and transverse magnetic (TM) polarized were simulated with Fimmwave. The beam-waist, w_0, of the mode along the horizontal and the vertical direction are reported in Table I. A mode matched SU8-polymer waveguide of refractive index n = 1.57 edge coupled to the laser waveguide was dimensioned by simulation. The polymer waveguide was sitting on a 3 μm thick SiO_2 (oxide) cladding, for optical insulation to the Si substrate, and surrounded by air at the sidewalls and on top. The highest light coupling efficiency, η, was calculated to be 90.5 % for a 1 μm thick and 3.2 μm wide polymer waveguide. The light transmission into the fundamental mode TM of the polymer waveguide was T ~75 % and the reflectivity at the facet of the laser was estimated of R ~15.5 %. The light loss in the edge-coupling is due by not perfect matching of the modes in the laser and in the polymer waveguide. The energy loss goes into higher order modes of the polymer waveguide. The engineering of a cladded polymer waveguide can increase the coupling efficiency.

The facet of the laser is spaced from the sidewall by a distance d, and the polymer infills this spacing. In this case the Rayleigh range, Z_R, can be calculated to roughly estimate the light coupling loss given by d. Z_R was calculated for the vertical component of the laser beam as it has the narrower waist and the largest divergence. For a gaussian beam with waist of $w_0 = 0.578$ μm, the Rayleigh range of the beam is:

$$Z_R = \frac{\pi \cdot w_0^2 \cdot n}{\lambda_0} = 1.23\mu\text{m} \quad (1)$$

where n is the refractive index of the SU8-polymer and λ_0 is the wavelength of the light. This means that the edge-coupling studied can be estimated tolerant to longitudinal misalignment of up to ~1.2 μm.

The simulation of the lateral and vertical misalignment shows a <1 dB loss in coupling efficiency for $\Delta x < 0.7\mu$m and $\Delta y < +0.2$ μm and $\Delta y < -0.7\mu$m respectively [Fig. 2]. The asymmetric behavior of the light coupled when moving the laser vertically [Fig. 2(b)] is due to the geometry of the system with the cladding below the polymer waveguide and the air on top of it.

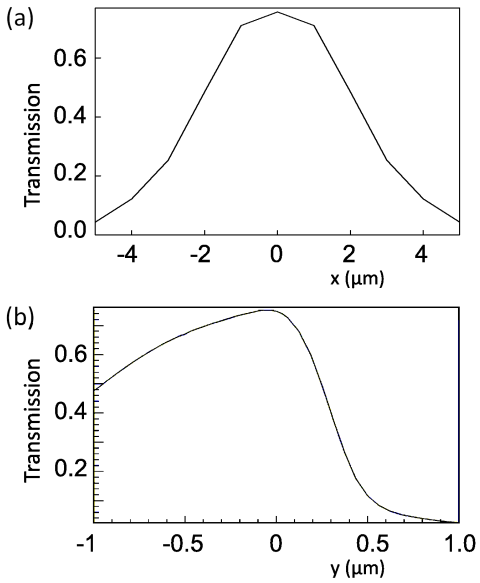

Fig. 2. (a) Study of the fundamental mode *TM* transmission from the laser to the polymer waveguide versus lateral and (b) vertical misalignment (in μm) simulated with LUMERICAL and FIMMWAVE.

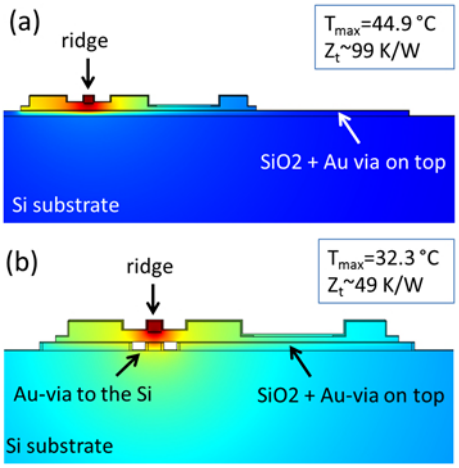

Fig. 3. Diagram of the thermal sink simulated with COMSOL, (a) for the O-band laser integrated in the recess on top of a metal thermal via and (b) for the same laser with a modified thermal via that shortens the heat path to the sink. The Z_t drops from 90 to 45 K/W.

C. Thermal Model

A thermal model of the laser integrated in the SOI recess using COMSOL [32] provides a simulated thermal impedance of Z_t ~99 K/W [Fig. 3(a)] while the same laser printed on the surface of the SOI would result in a higher thermal impedance of Z_t ~132 K/W. A metal via under the laser that sinks the heat to the substrate with a shorter path reduces Z_t to 49 K/W [Fig. 3(b)]. Simulations also suggest that an increase in the thickness of the metal layer used for thermal via reduces the thermal impedance by a few K/W, and it is less effective when sinking the heat far from the active region of the device. Only

the thermal via proposed in Fig. 3(a) was applied in this work as printing on metal layers with topography has not yet been explored.

III. Experimental Methods

O-band InP lasers were integrated into recesses fabricated on a SOI wafer by μTP with the strategy of Fig 1(d). The μTP process involved shearing the coupon to a sidewall of the recess while in gentle contact to the bottom of the recess and then bonding the coupon when matched to the sidewall. The method removes longitudinal misalignment and rotation. The lateral alignment to the pre-defined SOI waveguide is determined by the tolerances of the μTP technique [24] which depend sensibly on the application of pattern recognition techniques. A calibrated thickness metal layer deposited at the bottom of the recess allowed accurate vertical alignment of the lasers to the SOI waveguiding layer. The same metal layer has been proven to work as electrical contact and has the potential to work as an effective thermal via as analyzed in the previous section. A polymer waveguide was aligned to the laser waveguide while achieving full butt-coupling. The polymer waveguide was further aligned to a tapered SOI waveguide.

A. Laser Devices

550 μm long and 60 μm or 80 μm wide micro-transfer-printable laser coupons were fully pre-fabricated on the source InP wafer as dense arrays of about 1,000 devices per cm^2. A 500 μm long Fabry-Perot cavity was defined by two dry etched facets and passivated by an optically neutral SiO_2 layer and the back facet was then coated with a reflective metal layer. A 2 μm wide ridge etched just above the active region provides the lateral confinement of the light for single mode output. Accessible P- and N-type metal contacts were defined for testing the devices before and after transfer. The fabrication of the lasers included the steps for preparing the coupons to the undercut and the μTP as shown in our previous work [20], [38]. The coupons were released from their native substrate by selectively etching a 500 nm thick InAlAs sacrificial layer below the N-InP cladding with $FeCl_3$:H_2O (1:2). The resulting suspended devices were then picked up and transfer-printed epitaxial-side-up to the pre-fabricated recesses on the SOI.

B. SOI Platform

A 220 nm SOI layer on a 3 μm thick buried oxide cladding was patterned to create an array of 1.57 μm deep rectangular recesses suitable for edge coupling to waveguides [Fig. 4, Fig. 5]. Electron-beam (e-beam) lithography and a Cl-based dry-etch were used to define the profile of the recesses and some 0.6 μm wide SOI waveguides for optical connection [Fig. 4(a)]. Tapers with a 140 nm wide tip were defined at the end of each SOI waveguide for evanescent light coupling with the polymer waveguides. A second CF_4:CHF_3-based dry-etch formed the recesses in the SiO_2 with $\pm$0.03 μm tolerance on the targeted etch depth and without reaching the substrate

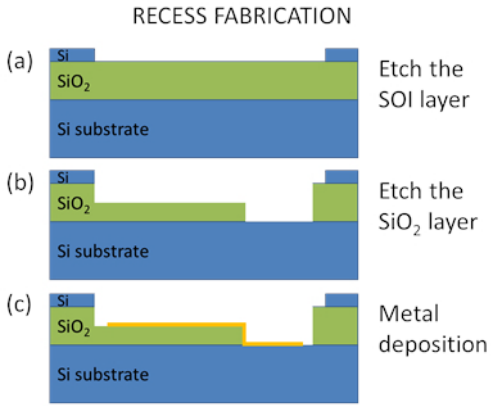

Fig. 4. (a) The recesses were fabricated by dry-etching the SOI layer, (b) the oxide (without reaching the Si substrate) and a recess to the Si substrate; (c) then a metal layer is evaporated to adjust the recess depth and sinks the heat to the substrate.

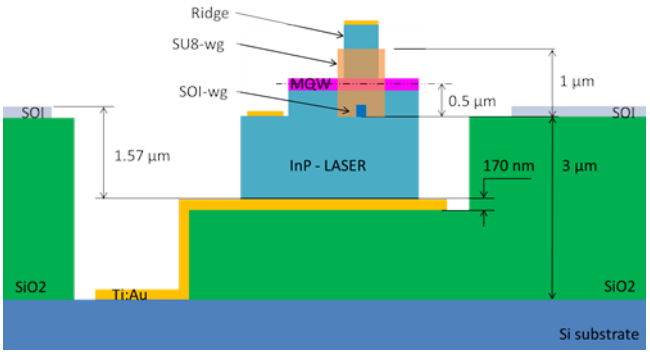

Fig. 5. Cross section of a 1.57 μm deep recess formed in the buried oxide to accommodate the laser. The 170 nm thick metal layer allows tuning the height of the active region to be 0.5 μm above the top of the oxide layer. Then a 1 μm thick patterned SU8 waveguide is edge coupled to the laser waveguide.

[Fig. 4(b)]. A third patterning and dry-etch opened part of the recesses created to access the Si substrate close to the printing area of the device [Fig. 4(b)]. A 1 Å/s slow-rate flat evaporation of a Ti:Au (10:110) nm followed by a slow-rate (1 Å/s) 360° angled Ti:Au (10:40) nm evaporation defined a smooth flat metal layer suitable for adhesive-less printing at the bottom of the recess [Fig. 4(c)] and the thermal via for the heat sink. A high flatness and smoothness of the underlying SiO_2 surface is crucial to prevent defect formation on the metal layer. Presence of imperfections and debris on the metal surfaces require thick adhesive layers. The resulting metal surface shows flatness of $<$0.03 nm/μm and nominal roughness of $<$1 nm. The metal layer thickness can be tuned with $\pm$10 nm accuracy and allows alignment of the active region of the device to the SOI and the polymer waveguide along the vertical axis.

C. μTP of the Laser Into the Recess on the SOI

The pre-released InP lasers were heterogeneously integrated to the recesses fabricated on the SOI wafer by μTP in full manual mode and without using alignment marker and pattern recognition. The robotic arm of the transfer printer

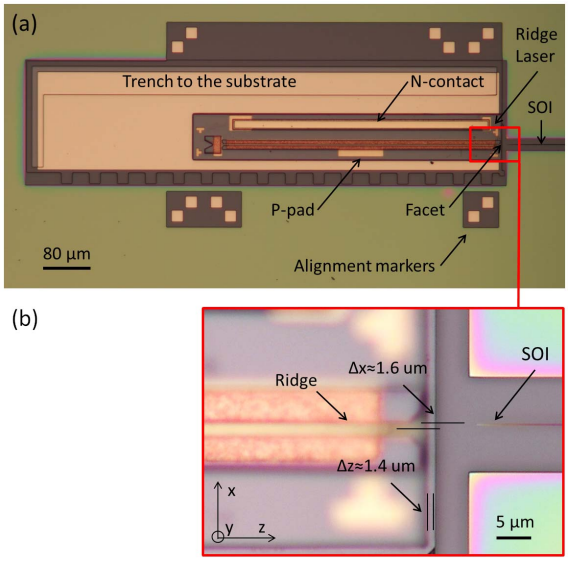

Fig. 6. (a) Digital microscope image of a laser printed in a type 2 recess in the SOI. (b) A zoom on the emitting facet shows a misalignment of $\Delta x \sim 1.6$ μm and $\Delta z \sim 1.4$ μm to the SOI given by the encapsulation ledge.

brought the coupons to <0.1 μm distance from the metal layer, then they were moved to the sidewall of the recess and matched to it removing any longitudinal misalignment and rotation of the coupon to the SOI. Finally, they were printed onto the metal layer. Even if the integrated laser coupon was completely matched to one of the sidewalls [Fig. 6(a)], the facet was recessed by $\Delta z = 1.4$ μm to the sidewall as a 1.4 μm wide ledge was defined around the coupon for the encapsulation [Fig. 6(b)]. The lateral alignment of the emitting facet to the SOI was measured at $\Delta x = 1.6$ μm [Fig. 6(b)], which can be improved through a pattern-recognition-based alignment. The vertical alignment to the SOI was determined of Δy <30 nm due to the tolerance of the etch depth along the SOI chip. The application of a nanometer scale thin vapor coated hexamethyldisilazane (HMDS) layer inside the recesses before the μTP helped to keep the printing yield high (100%) as observed when printing an array of 20 devices on an Au coated Si substrate.

D. Polymer Waveguide

A straight polymer waveguide was defined post-integration on top of the SiO_2 cladding and edge coupled to the laser and evanescent coupled to the tapered SOI waveguide [Fig. 7, Fig. 8]. This was achieved by spinning a SU8 polymer layer of 1.5 μm thickness on the SOI after printing the devices in the pre-fabricated recesses. The thickness targeted was 1 μm with the difference between expected and actual thickness due to the topography present on the SOI. An etch-back of the polymer will bring the height of the waveguide back to 1 μm. E-beam lithography was used to define a 7.5 μm wide and 2 mm long waveguide edge coupled to the ridge of the laser with <0.7 μm misalignment [Fig. 7(a)]. Full butt-coupling of the polymer waveguide to the facet of the laser was achieved despite the 1.4 μm spacing between the facet and the sidewall of the recess [Fig. 7(b, c)], with the coupon

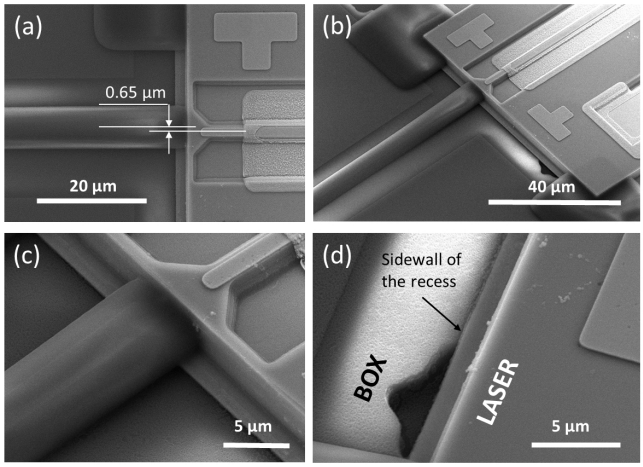

Fig. 7. Scanning electron microscopy images (a) of the waveguide aligned to the ridge of the laser with <0.7 μm lateral misalignment, (b, c) complete butt coupling to the facet and (d) full match of the laser coupon to the sidewall of the recess created into the buried oxide layer (BOX).

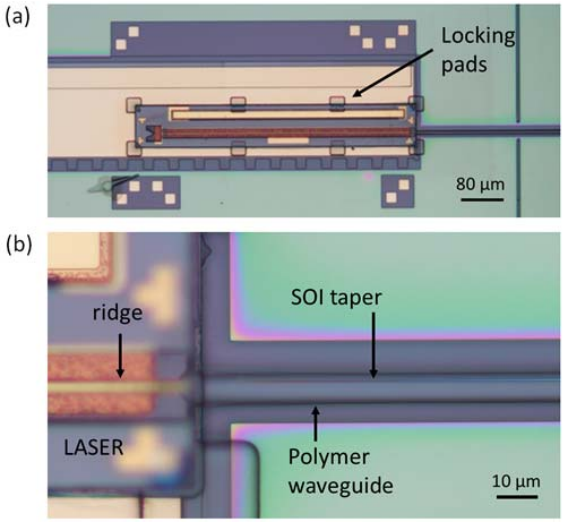

Fig. 8. (a) Digital microscope image of the InP laser printed in a recess on the SOI and edge coupled to the polymer waveguide. (b) A zoom-in on the polymer waveguide connection allows visualize the SOI tapered waveguide positioned 4.75 μm far from the edge of the recess.

completely matched to the sidewall [Fig. 7(d)]. The spacing allowed for full light transfer to the waveguiding section as estimated in paragraph B of the previous section ($d_{max} \sim 2.4$ μm). The polymer waveguide incorporated a parallel SOI waveguide with the taper positioned at 4.75 μm from the edge of the recess [Fig. 8(b)]. The misalignment of the polymer waveguide to the SOI waveguide was $\Delta x \sim 2.25$ μm, given by the sum of the misalignment to the laser waveguide (0.65 μm) and of the laser to the SOI (1.6 μm). The second end of the waveguide lands in another recess aligned to the first. Additional pads around the coupon were defined with the polymer layer for locking the device in place in case further processing on the sample could affect the adhesion to the substrate [Fig. 8(a)].

IV. Experimental Results

The integrated devices were characterized electrically and spectrally before and after μTP to the recess and after

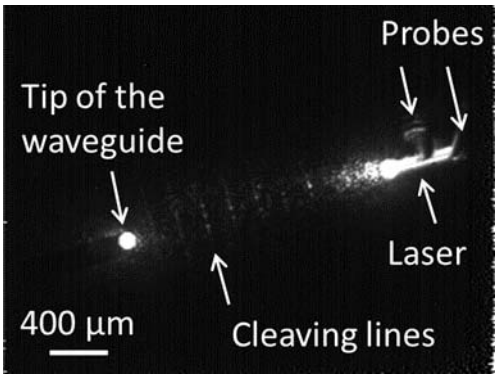

Fig. 9. IR camera imaging of the laser operating on the SOI and coupled to the 2 mm long polymer waveguide, the light comes out at the free end of the waveguide with a bright spot. Some transverse cleaving lines etched beside the waveguide for following cleaving of the chip reflect the light dispersed beside the laser coupon.

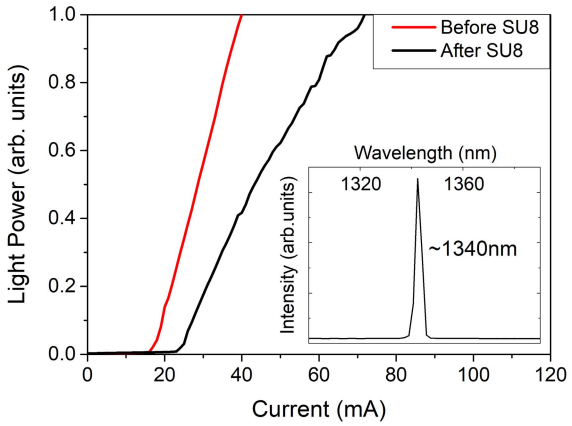

Fig. 10. L-I characteristics for the laser printed in the recess before and after coupling the light to the SU8 waveguide. The inset shows the emission wavelength of ∼1340 nm for the laser operating at 20°C before transfer.

edge-coupling to the polymer waveguide. The light coupling from the laser to the polymer waveguide and the SOI waveguide was detected with an infrared (IR) camera that shows the light coming out at the end of the 2 mm long polymer waveguide [Fig. 9].

The light-current (L-I) characteristics of the devices show a threshold current of I_{th} ∼17 mA before and after μTP to the SOI. I_{th} rises to ∼23 mA after coupling the light to the SU8 waveguide [Fig. 10] due to reduced reflectivity on the front mirror from R ∼32 % (in air) to R ∼15.5 %. The intensities of the two L-I curves are not related in the graph as the light was collected at an angle to the SOI chip, the decreased light power measured after the butt coupling of the polymer waveguide highlights the light is coupling into the waveguide and does not diverge as when the laser emits in air. The series resistance of the laser was measured of ∼14 Ω. The thermal impedance of the laser was measured of Z_{EXP} ∼116 K/W. The laser operating on the original InP substrate at 20 °C emits light at ∼1340 nm wavelength [Fig. 10, inset].

V. Conclusion

We reported the edge-coupling of an O-band etched facets InP laser to a polymer waveguide. Lasers were heterogeneously integrated into recesses of calibrated depth fabricated into the SOI by μTP. The integration layout was designed and dimensioned starting from the study of the light coupling by simulation. The strategy allows heterogeneous integration of pre-determined thickness InP transfer printable devices in a desired location and on the desired layer of the SOI. Fine vertical alignment of the laser waveguide to the SOI and thermal sink are achieved through an intermediate metal layer of calibrated thickness deposited at the bottom of the recess and connected to the Si substrate. Longitudinal alignment and rotation are improved by matching the coupon to one of the sidewalls of the recess. A layout for the improvement of the thermal via was simulated with COMSOL and proposed here. Alignment markers and pattern recognition have to be applied for improved lateral alignment.

A path for the application of μTP to the micro assembly of pre-fabricated InP optical functions to silicon photonics by edge coupling the light to polymer waveguides has been demonstrated in this work. The strategy enables the creation of PICs based on polymer or hybrid polymer-SOI waveguides interconnects.

Aknowledgement

We thank Dr. Francesco Floris from the photonics packaging group at Tyndall National Institute for the support provided during the simulations with LUMERICAL.

References

[1] D. Liang and J. E. Bowers, "Recent progress in lasers on silicon," *Nature Photon.*, vol. 4, pp. 511–517, 2010.
[2] D. Thomson *et al.*, "Roadmap on silicon photonics," *J. Opt.*, vol. 18, no. 7, 2016, Art. no. 073003.
[3] Z. Wang *et al.*, "Novel light source integration approaches for silicon photonics," *Laser Photon. Rev.*, vol. 11, no. 4, 2017, Art. no. 1700063.
[4] L. Carroll *et al.*, "Photonic packaging: Transforming silicon photonic integrated circuits into photonic devices," *Appl. Sci.*, vol. 6, no. 12, p. 426, 2016.
[5] S. Iadanza *et al.*, "Thermally stable hybrid cavity laser based on silicon nitride gratings," *Appl. Opt.*, vol. 57, no. 22, pp. E218–E223, 2018.
[6] A. P. Bakoz *et al.*, "Wavelength stability in a hybrid photonic crystal laser through controlled nonlinear absorptive heating in the reflector," *Light, Sci. Appl.*, vol. 7, pp. 1–7, Jul. 2018.
[7] A. J. Zilkie *et al.*, "Power-efficient III-V/Silicon external cavity DBR lasers," *Opt. Express*, vol. 20, no. 21, pp. 23456–23462, 2012.
[8] H. Guan *et al.*, "Widely-tunable, narrow-linewidth III-V/silicon hybrid external-cavity laser for coherent communication," *Opt. Express*, vol. 26, no. 7, pp. 7920–7933 2018.
[9] S. Lin *et al.*, "Vertical-coupled high-efficiency tunable III-V-CMOS SOI hybrid external-cavity laser," *Opt. Express*, vol. 21, no. 26, pp. 32425–32431, 2013.
[10] Y. Aoki, T. Kato, R. J. Mizuno, and K. Iga, "Micro-optical bench for alignment-free optical coupling," *Appl. Opt.*, vol. 38, no. 6, pp. 963–965, 1999.
[11] G. Roelkens *et al.*, "III-V/silicon photonics for on-chip and intra-chip optical interconnects," *Laser Photon. Rev.*, vol. 4, no. 6, pp. 751–779, 2010.
[12] B. Song, C. Stagarescu, S. Ristic, A. Behfar, and J. Klamkin, "3D integrated hybrid silicon laser," *Opt. Express*, vol. 24, no. 10, pp. 10435–10444, 2016.
[13] A. W. Fang, H. Park, O. Cohen, R. Jones, M. J. Paniccia, and J. E. Bowers, "Electrically pumped hybrid AlGaInAs-silicon evanescent laser," *Opt. Express*, vol. 14, no. 20, pp. 9203–9210, 2006.

[14] M. Lamponi *et al.*, "Low-threshold heterogeneously integrated InP/SOI lasers with a double adiabatic taper coupler," *IEEE Photon. Technol. Lett.*, vol. 24, no. 1, pp. 76–78, Jan. 2012.

[15] B. B. Bakir *et al.*, "Electrically driven hybrid Si/III-V lasers based on adiabatic mode transformers," *Proc. SPIE*, vol. 7719, May 2010, Art. no. 77191F.

[16] A. W. Fang *et al.*, "Integrated AlGaInAs-silicon evanescent racetrack laser and photodetector," *Opt. Express*, vol. 15, no. 5, pp. 2315–2322, 2007.

[17] B. Corbett, R. Loi, W. Zhou, D. Liu, and Z. Ma, "Transfer print techniques for heterogeneous integration of photonic components," *Prog. Quantum Electron.*, vol. 52, pp. 1–17, Mar. 2017.

[18] J. Justice, C. Bower, M. Meitl, M. B. Mooney, M. A. Gubbins, and B. Corbett, "Wafer-scale integration of group III–V lasers on silicon using transfer printing of epitaxial layers," *Nature Photon.*, vol. 6, no. 9, pp. 610–614, 2012.

[19] H. Yang *et al.*, "Transfer-printed stacked nanomembrane lasers on silicon," *Nature Photon.*, vol. 6, no. 9, p. 615–620, 2012.

[20] R. Loi *et al.*, "Transfer printing of AlGaInAs/InP etched facet lasers to Si substrates," *IEEE Photon. J.*, vol. 8, no. 6, pp. 1–10, Dec. 2016.

[21] J. Zhang *et al.*, "Transfer-printing-based integration of a III-V-on-silicon distributed feedback laser," *Opt. Express*, vol. 26, no. 7, pp. 8821–8830, 2018.

[22] A. De Groote *et al.*, "Transfer-printing-based integration of single-mode waveguide-coupled III-V-on-silicon broadband light emitters," *Opt. Express*, vol. 24, no. 13, pp. 13754–13762, 2016.

[23] L. Liu *et al.*, "Low-power-consumption optical interconnect on silicon by transfer-printing for used in opto-isolators," *J. Phys. D, Appl. Phys.*, vol. 52, no. 6, 2018, Art. no. 064001.

[24] D. Gomez *et al.*, "Process capability and elastomer stamp lifetime in micro transfer printing," In *Proc. IEEE 66th Electron. Components Technol. Conf. (ECTC)*, Jun. 2016, pp. 680–687.

[25] J. Yoon, S.-M. Lee, D. Kang, M. A. Meitl, C. A. Bower, and J. A. Rogers, "Heterogeneously integrated optoelectronic devices enabled by micro-transfer printing," *Adv. Opt. Mater.*, vol. 3, no. 10, pp. 1313–1335, 2015.

[26] A. Carlson, A. M. Bowen, Y. Huang, R. G. Nuzzo, and J. A. Rogers, "Transfer printing techniques for materials assembly and micro/nanodevice fabrication," *Adv. Mater.*, vol. 24, no. 39 pp. 5284–5318, 2012.

[27] M. A. Meitl *et al.*, "Transfer printing by kinetic control of adhesion to an elastomeric stamp," *Nature Mater.*, vol. 5, no. 1, pp. 33–38, 2006.

[28] C. A. Bower *et al.*, "Emissive displays with transfer-printed assemblies of 8 μm $\times$ 15 μm inorganic light-emitting diodes," *Photon. Res.*, vol. 5, no. 2, pp. A23–A29, 2017.

[29] R. Loi *et al.*, "Micro-transfer printing for advanced scalable hybrid photonic integration," in *Proc. Eur. Conf. Integr. Opt. (ECIO)*, 2018, pp. 98–100.

[30] J. Juvert *et al.*, "Integration of etched facet, electrically pumped, C-band Fabry–Pérot lasers on a silicon photonic integrated circuit by transfer printing," *Opt. Express*, vol. 26, no. 17, pp. 21443–21454, 2018.

[31] J. Juvert *et al.*, "Integration of III-V light sources on a silicon photonics circuit by transfer printing," in *Proc. IEEE 14th Int. Conf. Group IV Photon. (GFP)*, Aug. 2017, pp. 171–172.

[32] R. Loi *et al.*, "Thermal analysis of InP lasers transfer printed to silicon photonics substrates," *J. Lightw. Technol.*, vol. 36, no. 24, pp. 5935–5941, Dec. 15, 2018.

[33] R. Loi *et al.*, "Edge-coupling of O-band InP etched-facet lasers to polymer waveguides on SOI by micro-transfer-printing," in *Proc. Eur. Conf. Integr. Opt. (ECIO)*, 2019.

[34] Z. Zhang *et al.*, "Polymer-based photonic toolbox: Passive components, hybrid integration and polarisation control," *IET Optoelectron.*, vol. 5, no. 5, pp. 226–232, 2011.

[35] D. De Felipe *et al.*, "Recent developments in polymer-based photonic components for disruptive capacity upgrade in data centers," *J. Lightw. Technol.*, vol. 35, no. 4, pp. 683–689, Feb. 15, 2017.

[36] R. Dangel *et al.*, "Polymer waveguides for electro-optical integration in data centers and high-performance computers," *Opt. Express*, vol. 23, no. 4, pp. 4736–4750, 2015.

[37] S. Dhoore, S. Uvin, D. Van Thourhout, G. Morthier, and G. Roelkens, "Novel adiabatic tapered couplers for active III–V/SOI devices fabricated through transfer printing," *Opt. Express*, vol. 24, no. 12, pp. 12976–12990, 2016.

[38] J. O'Callaghan *et al.*, "Comparison of InGaAs and InAlAs sacrificial layers for release of InP-based devices," *Opt. Mater. Express*, vol. 7, no. 12, pp. 4408–4414, 2017.

Ruggero Loi was born in Cagliari, Italy, in 1980. He received the B.Sc. degree in computational physics and the M.Sc. degree in applied physics from the University of Cagliari in 2008 and 2013, respectively, and the Ph.D. degree in engineering science from the Tyndall National Institute, University College Cork, Ireland, in 2019. His research deals with the integration of III-V materials and devices onto Silicon photonics by micro transfer printing (μTP).

He is currently a Process Development Scientist at X-Celeprint Limited, Ireland. He authored more than 20 scientific publications in the field of heterogenous integration of III-V to different platforms by μTP, he was involved in the European project Top-Hit.

R. Loi has been a member of the Optical Society of America since 2017.

Simone Iadanza was born in Tradate, (Varese), Italy, in 1989. He received the B.Sc. degree in engineering physics and the M.Sc. degree in materials engineering and nanotechnology from the Politecnico di Milano, Italy, in 2012 and 2016, respectively. He is currently pursuing the Ph.D. degree in physics with the Centre for Advanced Photonics and Process Analysis, Cork Institute of Technology, Ireland. He is currently working on the European DANCeR and RedFinch projects. His research interests include nano-photonics, opto-electronics and nano-fabrication of photonic crystals, silicon photonics, and semiconductor lasers dynamics.

Brendan Roycroft was born in Ireland in 1970. He received the B.A.I. degree in microelectronic and electrical engineering, the B.A. degree in mathematics, and the Ph.D. degree in physics from Trinity College, Dublin, in 1993 and 1998, respectively. He then designed, fabricated, and tested laterally coupled twin ridge lasers at the Optoelectronic Research Centre, Tampere, Finland, and at the Universidad Carlos III de Madrid, Spain. Since 2001, he has been with the Tyndall National Institute and Centre for Telecommunication Value vertical-cavity surface emitting lasers (VCSELs), and novel telecom lasers.

James O'Callaghan was born in Cork, Ireland. He received the Ph.D. degree from the Department of Physics, University College Cork, in 2002, under the topic of Spatial Coherence in Gain Profiled Semiconductor Lasers. He worked for two years in the Department of Optoelectronics, Ulm, Germany, where he is developing methods of thermal management in VCSELs before returning to his native city of Cork to work in the Tyndall National Institute as a Staff Scientist. Since then, he has been involved in a wide range of projects from developing high brightness semiconductor lasers to telecom-based photonics devices, such as Mach–Zehnder modulators and etched facet tunable lasers. He is currently working of the development of photonics-based devices for micro transfer printing and their integration into photonic integrated circuits.

Lei Liu was born in Hubei, China, in 1988. He received the B.S. degree in physics from the Taiyuan University of Technology, China, in 2010, and the Ph.D. degree in microelectronics and solid-state-electronics from the Institute of Semiconductor, Chinese Academy of Sciences. He worked in the Wuhan Research Institute of Posts and Telecommunications, China, as a Research Engineer. In 2016, he joined the Tyndall National Institute, Ireland, as a Post-Doctoral Researcher. His research interests include III-V laser diodes and photodetectors, micro LEDs, MEMS devices and modules, and integrated optoelectronic circuits on silicon.

He is currently a Process Development Scientist at X-Celeprint Limited, focusing on integrated optoelectronic modules and systems by micro-transfer-printing (μTP) technology.

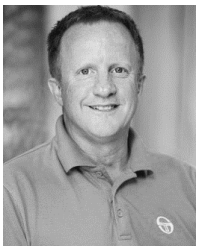

Kevin Thomas was born in U.K. in 1967. He received the B.Sc. degree in chemistry and the Ph.D. degree in surface chemistry and electron spectroscopy for chemical analysis from Cardiff University, U.K., in 1989 and 1994, respectively. From 1996 to 1998, he worked as a Production and Development Engineer in MOVPE with International Quantum Epitaxy (IQE), Cardiff. Since 1998, he has been a Research Scientist and Laboratory Manager in MOVPE and III-V material characterization at the Tyndall National Institute, University College Cork, Ireland.

Agnieszka Gocalinska was born in Poland in 1982. She received the M.Sc. degree in photonics from the Wrocław University of Technology, Poland, in 2005, and the Ph.D. degree in solid-state physics from the University of Cagliari, Italy, in 2010. She was a Marie Curie Fellow in frames of RTN Nanomatch in FP6. She currently works as a Research Scientist with the Epitaxy and Physics of Nanostructures Group, Tyndall National Institute, University College Cork, Ireland, where her main focus is epitaxy of III–V semiconductors for optoelectronic applications and quantum dots growth.

Emanuele Pelucchi was born in Milan, Italy. He received the M.Sc. degree from the Polytechnic of Milan and the Ph.D. degree from Bremen University and the TASC Laboratory, Trieste. In May 2006, he was awarded a SFI Principal Investigator Grant and moved to Tyndall National Institute in January 2007, where he set up a new research group in the field of III-V epitaxy for device applications, semiconductor (site-controlled) quantum dots and their applications to quantum optics and information. He has very broad interests, spanning from surface science and epitaxy to quantum optics. He has developed world leading III-V material quality (especially in the field of photonic integration) and growth process understanding, while uniquely developing and demonstrating arrays of site-controlled quantum dots and entangled photon emitters.

Alexander Farrell was born in Manchester, U.K., in 1992. He received the B.Sc. degree in environmental science from the Cork Institute of Technology in 2014 and the M.Sc. degree in analytical chemistry at UCC in 2015. His work deals with the heterogenous integration of photonic and electronic devices to different platforms by μTP. He currently works as Process Engineer Scientist at X-Celeprint Limited.

Steven Kelleher was born in Cork, Ireland, in 1990. He received the B.Sc. degree in electronic systems engineering from the Cork Institute of Technology, Ireland, in 2012, and the M.Sc. degree in microelectronic design from University College Cork, Ireland, in 2014. He currently works as Process Development Engineer at X-Celeprint Limited. His work involves the heterogenous integration of millimeter and micron scale devices, μTP application development, and software development.

Raja Fazan Gul was born in Islamabad, Pakistan. He received the B.S. degree in applied physics from Federal Urdu University (FUUAST), Islamabad, Pakistan, and the M.Sc. degree in energy science and technology from Ulm University, Ulm, Germany. He is currently leading projects as a Process Development Engineer at X-Celeprint Limited. He has worked extensively in the domain of semiconductor device fabrication. He has generated new ideas, designed devices and taken multiple devices from concept to fabrication and integration using transfer printing to rigid/flexible substrates.

His main interests include process development, design, and semiconductor device fabrication and heterogeneous integration via micro-transfer-printing.

António José Trindade was born in Portugal in 1985. He received the master's degree in physics engineering from the University of Aveiro and the Ph.D. degree in applied physics from the University of Strathclyde, Glasgow. He has work extensively on Organic Light Emitting Devices (OLEDs) and Organic Photovoltaics (OPVs). He has researched micron-size nitride-based micro-LED performance and transfer-printing technologies in the University of Strathclyde. He has worked extensively on different device architectures and taken multiple devices from concept to fabrication/integration and testing onto rigid/flexible substrates. He is currently a Product Development Scientist at X-Celeprint Limited.

His main interests include the performance optimization of light-emitting semiconductors and micro-displays, heterogeneous integration via micro-transfer-printing and process development.

David Gomez received the B.Sc. degree in materials science and engineering from the Massachusetts Institute of Technology. He is currently the Director of print services for X-Celeprint Limited. In this role, he works to further develop the print process for various custom applications for specific customers. He spent the first 15 years of his career working in high volume manufacturing facilities working for Freescale and Qimonda. Within that time, he has held positions both as an engineer and an engineering manager. He has spent the last five years working on managing and improving the micro-transfer print process both at Semprius and X-Celeprint Limited.

Liam O'Faolain was born in Cork, Ireland. He received the Ph.D. degree from the University of St. Andrews in Scotland. In 2012, he joined the group of Prof. David A. B. Miller, Stanford University, as an SU2P Entrepreneurial Fellow before returning to take up a lecturing position at St Andrews in 2013. In 2016, he re-located his research group to the Centre for Advanced Photonics and Process Analysis, Cork Institute of Technology. He is one of the leading authorities on disorder and loss in photonic crystal waveguides and has designed and realized the world's best slow light waveguides to date. His research group works on a range of projects using nano-photonics, hybrid lasers and integrated optics for applications in optical communications and optical sensing. He has authored or coauthored more than 100 journal articles.

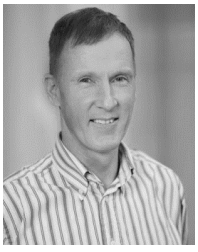

Brian Corbett received the B.Sc. degree in experimental physics and mathematics and the M.Sc. degree from Trinity College, Dublin, Ireland. He is currently a Senior Research Scientist and the Head of the III–V Materials and Devices Group, Tyndall National Institute, and also with the Center for Telecommunication Value Driven Research (CTR), Cork, Ireland. He has been engaged in developing extensive III–V micromachining expertise using dry and wet-etching techniques. This technology has been applied in both InP- and GaAs-based layer structures for devices such as low-cost single-frequency lasers as well as novel devices such as resonant cavity LEDs and photodetectors. His main research interest is in the use of geometry to define the optical properties of devices.